On the Magnetic Alignment of Metal Ions in a DNA-Mimic Double Helix

Hou Yu Zhang, Arrigo Calzolari, and Rosa Di Felice*

National Center on nanoStructures and bioSystems at Surfaces (S3) of INFM−CNR, c/o Dipartimento di Fisica, Università di Modena e Reggio Emilia, Via Campi 213/A, 41100 Modena, Italy

Received: April 28, 2005; In Final Form: June 12, 2005

We computed by spin-polarized DFT the structure and the electronic properties of an infinite periodic wire constituted of planar Cu-bridged hydroxypyridone chelator base pairs and of a similarly stacked finite dimer. The Cu centers undergo electronic hybridization with the bases. There is an unpaired spin per plane, and the majority-spins manifest ordering: The ferromagnetic and antiferromagnetic phases are energetically degenerate. The total magnetization of the ferromagnetic wire depends linearly on the number of planes in the stack. The combination of interplane spin coupling and intraplane metal−hydroxypyridone coupling makes this system very appealing for electronic and magnetic device exploitation.

The manipulation of DNA duplexes with metal ions is currently being explored as a viable route to replace hydrogen-bonding selectivity[1,2] and to impart an electrical function[2,3] to these biomolecules for exploitation in the nanotechnology framework. The use of redox-active cations to the latter purpose is particularly appealing because they coexist abundantly with biomolecules and are potential candidates to strongly alter the electronic structure of DNA polymers. Tanaka and co-workers[2] recently demonstrated the successful incorporation of Cu(II) ions in DNA oligoduplexes, mediated by modified bases: one to five consecutive planes along the helices were substituted by Cu-bridged hydroxypyridone pairs and decorated by Watson−Crick GC pairs at the edges of the short stacks. Electron paramagnetic resonance (EPR) spectra showed that the Cu centers hosted aligned spins with a ferromagnetic (FM) motif. Here, we present the theoretical description of the system, disclosing the electronic fingerprints of the electronic and magnetic coupling.

Because of the peculiar properties of recognition, structuring, and information storage, DNA molecules are attracting the attention of scientists worldwide and are catalyzing a huge interdisciplinary research effort toward the identification of novel materials for biotemplated nanotechnology[4,5] driven by supramolecular chemistry.[6] The high structural and chemical flexibility of DNA and its affinity to several biological and inorganic partners determine its capability to assume very complex one-to-three-dimensional conformations. Also, it was recently demonstrated that the precisely selective structuring and recognition of DNA double helices are not destroyed if suitable modified nucleobases are incorporated into short oligomers.[1,7] Such studies opened the way to the exploration of nucleobase mimics as an expansion of the genetic alphabet.

What is still lacking in DNA to realize the perfect candidate for an efficient nanoelectronic concept is the ability to conduct electrical signals. In fact, experiments performed so far to measure the dc conductivity of various DNA molecules revealed a very complex scenario.[8−12] Recent reviews[13−15] summarized that single short oligomers suspended between metal electrodes may be conductive, whereas long polymers deposited on an inorganic surface are insulating, unless they form networks or bundles. To install a sizable carrier mobility in long molecules, metal manipulation is attempted according to different schemes. On one hand, the DNA can be used to template the deposition of metallic wires.[8] On the other hand, metal manipulation can be directed for the metal to be accommodated inside the helical motif along the axis.[2,3] Whereas the former strategy results in nanowires much thicker than natural DNA (around 50 nm) and destroys the biological supramolecular capabilities, the latter procedure would give very thin nanowires of approximately the same diameter of the DNA molecules themselves and may be designed to maintain recognition.

The two frameworks for DNA maneuvering introduced above (i.e., metal insertion into the base core and design of alternative nucleobases) can be combined into a synergistic approach to synthesize double helices in which metal ions are aligned along the axis through alternative base pairing mediated by nucleoside mimics. It was thus shown that metal coordination can successfully replace the hydrogen-bonding pairing pattern[2,16] while preserving the helical structure and the autorecognition feature which are essential to DNA supramolecular chemistry and assembly. Whereas metal incorporation inside the base stack is routinely achieved in G4 quadruple helices constituted of the native guanine base,[17−19] alternative chelator nucleosides (also coined *ligandosides*[20]) have been employed to insert metal ions into double helices. We consider the case in which the chelator is hydroxypyridone (hereby labeled **H**) and the metal is Cu.[2] By means of state-of-the-art quantum mechanical simulations, we discuss the electronic coupling between the inner metal and the surrounding **H** molecules and show that this occurs through the appearance of hybrid frontier orbitals. In addition to this charge interaction that might be the basis for enhanced carrier mobility through the helix, we show the fingerprints of spin alignment.[2]

Our simulations are based on periodic-supercell plane-wave ultrasoft-pseudopotential[21] spin-polarized density functional theory employing the PW91 exchange-correlation functional and the PWSCF package of computer codes (http://www.pwscf.org). The plane-wave kinetic-energy cutoff was 25 Ry and a single special **k** point was used in sums over the one-dimensional Brillouin zone. A recent study of guanine quadruplexes[18]

* Author to whom correspondence should be addressed. Phone: +39-059-2055320; fax: +39-059-2055651; e-mail: rosa@unimore.it.

10.1021/jp052202t CCC: $30.25
Published on Web 07/22/2005

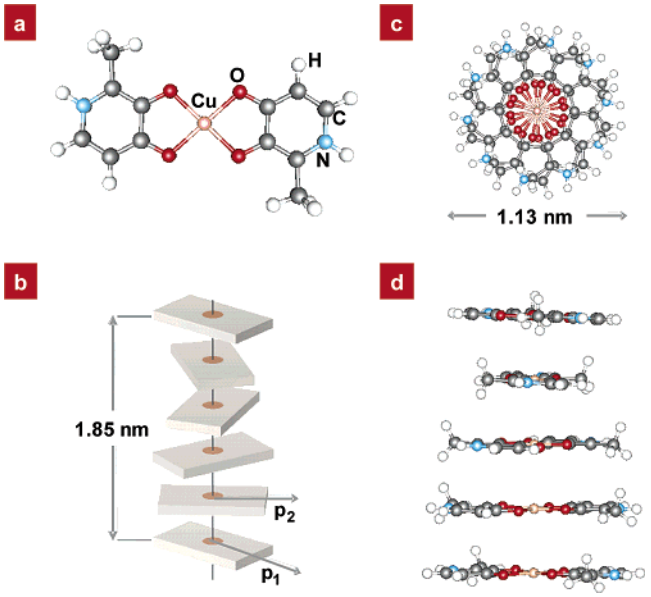

Figure 1. (a) Top-view ball-and-stick rendering of the equilibrium configuration (vanishing forces) for the planar building-block molecule **H**−Cu(II)−**H** in the trans conformation. The constituent **H** molecules are truncated at the joint of the sugar−phosphate backbone that is replaced by a H atom attached to each N atom. (b) Schematic model of the wire: each metalated pair **H**−Cu(II)−**H** is represented by a brick at which center the metal ion is marked by a colored circle. The vertical line is the axis of the double helix. The vectors $\mathbf{p_1}$ and $\mathbf{p_2}$ indicate the polar axes on two adjacent planes and form an angle of 36°. The replica (top brick) of the basal plane (bottom brick) is included in the scheme to manifest the periodicity (which is half that of natural B-DNA because the two bases in each pair are equal). (c, d) Top-view and perspective ball-and-stick rendering for the [**H**−Cu(II)−**H**]$_5$ pentamer, which constitutes the periodicity unit of the infinite wire. The wire is labeled [**H**−Cu(II)−**H**]$_{5w}$.

guarantees the accuracy of our computational tools to describe helical arrangements of DNA bases. The ability of the method to treat Cu ions was proven in a study of the metalloprotein azurin.[22] The **H**−Cu(II)−**H** planar building block (Figure 1a) and the [**H**−Cu(II)−**H**]$_2$ stacked dimer are simulated by supercells 23.5 × 23.5 × 13.5 Å^3 and 23.5 × 23.5 × 16.0 Å^3 wide, respectively (containing a minimum vacuum thickness of 10 Å separating neighboring replicas). According to the experimental characterization,[2] adjacent planes are rotated by 36° and are separated by a distance of 3.7 Å. The infinite wire is constructed through periodic replication of the [**H**−Cu(II)−**H**]$_5$ stacked pentamer (Figure 1c, d): Because of the equivalence of the two **H** bases in each Cu-mediated pair, the helical symmetry is reproduced with five planes instead of the ten planes as in Watson−Crick pairs formed by complementary bases. The formal electronic configuration of Cu(II) ions (neutral atom $3d^{10}4s^1$) in these neutral systems is $3d^9$. The structure of the **H**−Cu(II)−**H** plane is fully relaxed until the atomic forces vanish within 0.03 eV/Å. For the stacked assemblies, the geometry is not optimized, because DFT calculations at the present implementation stages are not able to predict the interplanar stacking distances because of the lack of van der Waals interactions. We do not include such effects through a parametric description;[23] hence, we do not attempt a structural prediction. Instead, we assemble the structures according to the experimental indications, verify that they are characterized by small atomic forces, and focus only on the electronic properties (unlikely to be strongly influenced by van der Waals interactions). Following experimental clues, we start with a guess magnetization on each plane to exit the paramagnetic local

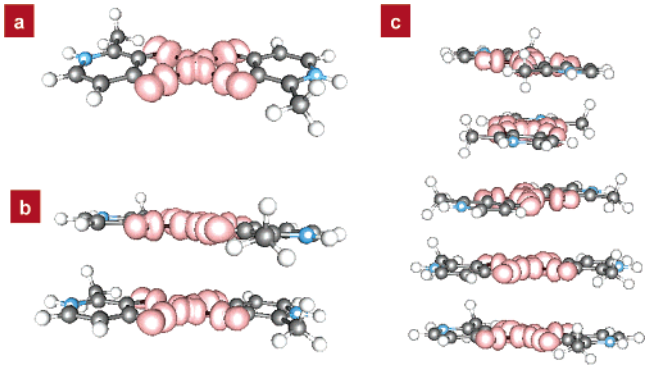

Figure 2. Isosurface plots of the spin density for the **H**−Cu(II)−**H** pair (a), the [**H**−Cu(II)−**H**]$_2$ dimer (b), and the [**H**−Cu(II)−**H**]$_{5w}$ periodic wire (c). The spin density is defined as $\rho_M-\rho_m$, where ρ_M (ρ_m) is the electronic charge summed over the majority-spin (minority-spin) orbitals. The spin density for the isolated plane has a σ-like hybrid Cu−O distribution. The σ character is with respect to both the molecular plane and the Cu−O bonds. For the dimer and the wire, the spin density clearly stems from the combination of the component planes, meaning that the stacking superposition is not able to alter the intraplane metal−base coupling, but for minor quantitative effects. The σ-like shape of the spin density for the [**H**−Cu(II)−**H**]$_{5w}$ periodic wire is likely to inhibit the behavior of similar extended molecules as π-ways for charge motion through the stack.

energy minimum, and then we compute the self-consistent electronic structure by relaxing all the degrees of freedom (within translational symmetry).

Figure 1 illustrates the simulated structures. In the zero-force geometry obtained for **H**−Cu(II)−**H**, the Cu(II)-bridged pair maintains an almost perfect planar shape: the highest out-of-plane deflection is 0.15 Å. The O atoms are symmetrically liganded to the central Cu(II) ion, at a distance of 1.95 Å (±0.02 Å): this value is typical of Cu(II)−ligand distances for strong ligands, in biomolecules where copper ions are naturally present,[22] as well as in artificial DNA-mimic double helices.[16] Force computations without full atomic relaxation reveal that the finite [**H**−Cu(II)−**H**]$_2$ dimer (Figure 2b) and infinite [**H**−Cu(II)−**H**]$_{5w}$ wire (Figure 1c, d) made of relaxed pairs at fixed interplane distance and rotation angle are very close to equilibrium; therefore, we conclude that the planarity and the Cu−O distance are maintained upon stacking, independently of the total length of the stack.

An interesting quantity that may be extracted from the computational output is the charge transfer between the metal and the liganded heterocycles, deduced from the atomic charges computed through the Löwdin population analysis. Such atomic charges are obtained through projections onto atomic orbitals, are not physically defined in a unique way, and may serve only for a qualitative analysis (see Supporting Information for more details). Relative to the free molecular phase, each **H** heterocycle in the **H**−Cu(II)−**H** pair loses a small fractional amount of electrons (∼0.15, which must be taken with caution and is intended only as a relative value with respect to the **H** gas phase), and this loss is mainly localized on the most electronegative atoms O and N. The heterocycles exhibit the same charge distribution in the isolated pair, in the dimer, and in the wire (see Supporting Information). The charge state of copper is the same in the pair and in the stacks, with positive charge much less than the nominal charge state 2+. This fractional charge on the metal is a first indication that the unpaired electron cannot be entirely localized on copper but is shared between the metal and the **H** molecules. Such a behavior is clearly demonstrated by the computed spin density: the isosurface plot

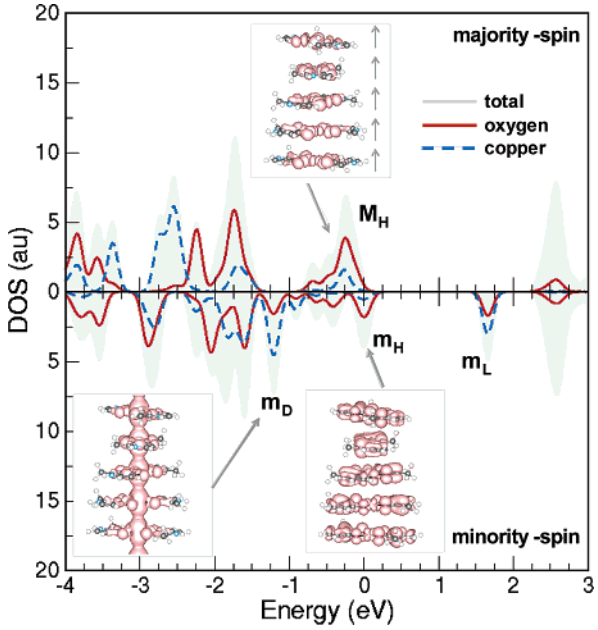

Figure 3. Total and atom-projected density of states for the periodic wire, computed with Gaussian spreading of the one-particle energy eigenvalues. The top (bottom) graph is obtained from the majority-spin (minority-spin) wave functions. The insets show selected frontier orbitals with σ and π character with respect to the molecular plane and a lower-energy orbital with axial charge delocalization induced by combined metal−metal and metal−hydroxypyridone coupling. The origin of the energy scale (horizontal axis) is set at the center of the highest occupied peak, so that the Fermi level of the system lies within the gap between m_H and m_L.

shown in Figure 2a reveals that the unpaired electron is indeed a σ-like antibonding hybrid resulting from Cu d and O p electron states.

Panels b and c of Figure 2 show that the unpaired spins are equally distributed across the planes. The computed total magnetization per cell is 1, 2, and 5 μ_B for the pair (Figure 1a), dimer (Figure 1b), and wire (Figure 1c). To bring insight into the details of electronic coupling, we carry out a full description of the electronic structure, accounting for the occupation of the energy levels. It is particularly interesting to inquire about the origin of the σ-shaped spin density, at odds with the common finding of a π HOMO for C-based aromatic cycles and heterocycles (including DNA bases[24,25]).

The analysis of the computed electronic structure is summarized in Figure 3 that shows the total and atom-projected density of states (DOS and PDOS, respectively) of the periodic wire $[\mathbf{H}-\mathrm{Cu(II)}-\mathbf{H}]_{5w}$ and significant single particle electron states. Most of the highest occupied energy levels do not manifest any band dispersion along the helical axis; hence, the energy diagram is given by discrete energy levels. Each peak in the DOS stems from one or more energy manifolds: each manifold is precisely constituted of five levels (thus, we call them quintuplets in the following), according to the molecular multiplicity in the pentameric periodicity unit of the wire. This behavior is quite clear at energies close to the forbidden gap (e.g., around the energy origin in Figure 3) but is less distinguishable at lower energies because of the coexistence of several hybridizing molecular orbitals and consequent quintuplet mixing; a similar behavior was already identified for a guanine quadruple helix with incorporated metal ions,[18] and the relation with the helical symmetry was commented elsewhere.[13]

Focusing around the forbidden gap, we point out that the highest occupied molecular quintuplet (peak m_H) contributes to the minority-spin DOS and is not singly occupied: its majority-spin counterpart with the same isosurface shape is embedded in peak M_H (at the high-energy edge of M_H). A similar behavior, with the minority-spins determining the highest energy occupied DOS peak,[26] was found in the native active site of the electron-transfer protein azurin.[22] This means that the highest occupied molecular orbitals (the inset pointing at peak m_H in Figure 3 shows an isosurface plot of the quintuplet convolution) are indeed π-like as expected for conjugated heterocycles. However, each constituent level has a majority-spin M_H counterpart and is accordingly doubly occupied (with a spin-up/spin-down splitting); therefore, these orbitals do not contribute to the spin density distribution. The unpaired electrons are instead grouped into a quintuplet at the low-energy edge of M_H, 0.3 eV below the peak m_H. The convolution of the constituent σ orbitals is shown as an isosurface plot in the inset in the top panel of Figure 3. The minority-spin counterpart is unoccupied and gives origin to peak m_L. This situation explains the σ-like character of the spin density, contrasting with the π-like nature of the HOMO. We highlight the presence of hybrid Cu−**H** orbitals giving peak m_D at 1.2 eV below m_H that exhibit delocalization along the wire axis accompanied by a band dispersion of 0.4 eV. The discussed DOS features m_D, m_H, and M_H have mixed Cu−O character, thus revealing efficient metal−base coupling.

In principle, the unpaired electrons residing on each plane of the wire could be oriented in an arbitrary way. Our results clearly show the presence of a quintuplet constituted of five singly occupied orbitals with all majority-spin electrons. Thus, the simulations reveal a ferromagnetic alignment consistent with the measured EPR spectra.[2] This evidence is further validated by the electronic structure of the $[\mathbf{H}-\mathrm{Cu(II)}-\mathbf{H}]_2$ dimer that exhibits an equilibrium magnetic structure. The computed total magnetization of the dimer (pentamer periodicity unit) is twice (5 times) that of the metalated pair, giving a linear scaling with the number of spins/planes and allowing to define an intrinsic quantity for stacks of arbitrary length, namely, the magnetization per plane. We remark that the inclusion of the backbone would not significantly modify our results: Gervasio and co-workers demonstrated that in double-stranded DNA only the counterions yield additional states in the gap,[27] whereas we recently verified for G4-DNA[28] that the backbone inserts a new manifold below the HOMO, without changing the amplitude and nature of the HOMO manifold and the fundamental band gap.

The computed data only demonstrate that the FM phase is metastable, but it cannot be concluded that it is the most favorable. To inquire about the stability of the various possible spin alignments, we performed similar calculations with a double supercell containing 10 planes of $\mathbf{H}-\mathrm{Cu(II)}-\mathbf{H}$ pairs (310 atoms). For this wire, (i) when we impose an equal starting magnetization on each plane, we end up with a ferromagnetic electronic configuration equivalent to that presented above, with a total magnetization per cell equal to 10 μ_B; and (ii) when we impose opposite starting magnetizations on adjacent planes (+1, −1), we end up with an antiferromagnetic (AM) electronic configuration, with a total magnetization per cell equal to 0. The total energies of the two phases are equal within the precision of the calculations, which means that collinear spin-polarized DFT ground-state simulations do not predict the ferromagnetic alignment as the most favorable product.[29] Of course, it could be prepared by suitable external conditions that are conducive to parallel spin coupling or even by the asymmetry of the synthesized molecules[2] because of the presence of native base pairs (that break the uniform sequence of **H**−Cu-

(II)−**H** pairs) at the ends of the stack. It is also interesting to analyze the electronic properties of the antiferromagnetic wire. We give the images of some relevant orbitals as Supplementary Information. Here, we just report the most remarkable characteristics. Differently from the FM phase, in the AM phase no splitting is revealed between spin-up and spin-down orbitals of a given type; for example, whereas for the ferromagnetic phase the spin-up orbital corresponding to peak m_H (Figure 3) is shifted to lower energies (see earlier discussion), for the antiferromagnetic phase the equivalent spin-up and spin-down HOMO peaks (isosurface plots in the Supplementary Information) are both found at the same energy of peak m_H.[30] The energy levels are all doubly occupied and are gathered in fivefold multiplets: each quintuplet contains 10 states, 5 spin-up and 5 spin-down, with opposite spins centered on alternate planes. The HOMO multiplet has a shape similar to peak m_H of Figure 3, with spin-up (spin-down) isosurfaces localized on odd (even) planes. Occupied and unoccupied σ states similar to peak M_H are found at energies −0.23 and 1.67 eV (the latter is the LUMO): those at −0.23 eV are spin-up (spin-down) on even (odd) planes, and in those at 1.67 eV the localization of spin-up and spin-down electrons is exchanged on odd and even planes.

Let us now comment on the meaning of the present findings. (i) The spin-coupling fingerprint of the wire indicates that stacks of **H**−Cu(II)−**H** mimetic pairs, which may be substituted to natural DNA base pairs at controlled locations along the double helix, are suitable to be prepared in a high-spin state. (ii) The nature of the σ and π frontier orbitals, with nodes between the stacked planes, does not support bandlike electron conduction. However, the efficient metal−base hybridization may suggest alternative mechanisms, for example, driven by a redox activity of the inner cations. (iii) The orbitals with continuous axial delocalization lying 1.2 eV below the top of occupied levels resemble a linear sequence of metal centers, templated and kept at the proper distance by the nucleobase arrangement that neutralizes the repulsive electrostatic interactions between adjacent ions. (iv) DFT-based first-principle calculations may have a strong impact in the design of novel DNA-mimic nanowires: although the technique is still limited in structural predictions, such hurdles can be overcome successfully with the aid of classical simulations to sample the phase space[31] and to choose relevant configurations for the deeper quantum mechanical investigations. (v) Since the metal−base hybridization is induced by the square-planar symmetry of the copper centers in the stack, we speculate that the qualitative features may be generalized to a broader class of systems characterized by pairs of aromatic chelators coordinated to Cu(II) ions through O linkers.

Acknowledgment. Anna Garbesi, Elisa Molinari, and Stefano Corni are gratefully acknowledged for stimulating discussions. Rita Stacchezzini provided valuable graphical aid. The work was funded by the EC through Contract IST-2001-38951 and by MIUR-IT through Project FIRB-NOMADE. Computer time at CINECA was provided by INFM through the Parallel Supercomputing Committee.

Supporting Information Available: (i) Charge population analysis, complemented by four figures (S1−S4) and one table that report the relative atomic charges; (ii) electronic properties of the antiferromagnetic phase, illustrated by two figures (S5, orbitals; S6, density of states). This material is available free of charge via the Internet at http://pubs.acs.org.

References and Notes

(1) Kool, E. T. *Acc. Chem. Res.* **2002**, *35*, 936−943.
(2) Tanaka, K.; Tengeiji, A.; Kato, T.; Toyama, N.; Shionoya, M. *Science* **2003**, *299*, 1212−1213.
(3) Rakitin, A.; Aich, P.; Papadopoulos, C.; Kobzar, Yu.; Vedeneev, A. S.; Lee, J. S.; Xu, J. M. *Phys. Rev. Lett.* **2001**, *86*, 3670−3673.
(4) Seeman, N. C. *Nature* **2003**, *421*, 427−431.
(5) Yurke, B.; Turberfield, A. J.; Mills, A. P., Jr.; Simmel, F. C.; Newmann, J. L. *Nature* **2000**, *406*, 605−608.
(6) Keren, K.; Krueger, M.; Gilad, R.; Ben-Yoseph, G.; Sivan, U.; Braun, E. *Science* **2002**, *297*, 72−75.
(7) Liu, H.; Gao, J.; Lynch, S. R.; Saito, Y. D.; Maynard, L.; Kool, E. T. *Science* **2003**, *302*, 868−871.
(8) Braun, E.; Eichen, Y.; Sivan, U.; Ben-Yoseph, G. *Nature* **1998**, *391*, 775−778.
(9) de Pablo, P. J.; Moreno-Herrero, F.; Colchero, J.; Gómez-Herrero, J.; Herrero, P.; Baró, A. M.; Ordejón, P.; Soler, J. M.; Artacho, E. *Phys. Rev. Lett.* **2000**, *85*, 4992−4995.
(10) Porath, D.; Bezryadin, A.; de Vries, S.; Dekker, C. *Nature* **2000**, *403*, 635−638.
(11) Fink, H.-W.; Schönenberger, C. *Nature* **1999**, *398*, 407−410.
(12) Kasumov, A. Yu.; Kociak, M.; Guéron, S.; Reulet, B.; Volkov, V. T.; Klinov, D. V.; Bouchiat, H. *Science* **2001**, *291*, 280−282.
(13) Porath, D.; Cuniberti, G.; Di Felice, R. In *Long-Range Charge Transfer in DNA*; Schuster, G., Ed.; Springer-Verlag: Heidelberg, Germany, 2004; Vol. 2, pp 183−228.
(14) Endres, R. G.; Cox, D. L.; Singh, R. R. P. *Rev. Mod. Phys.* **2004**, *76*, 195−214.
(15) Di Ventra, M.; Zwolak, M. DNA Electronics. In *Encyclopedia of Nanoscience and Nanotechnology*; Nalwa, H. S., Ed.; American Scientific Publishers: New York, 2004; Vol. 2, p 475.
(16) Atwell, S.; Meggers, E.; Spraggon, G.; Schultz, P. G. *J. Am. Chem. Soc.* **2001**, *123*, 12364−12367.
(17) Davis, J. T. *Angew. Chem., Int. Ed.* **2004**, *43*, 668−698.
(18) Calzolari, A.; Di Felice, R.; Molinari, E.; Garbesi, A. *J. Phys. Chem. B* **2004**, *108*, 2509−2515; *J. Phys. Chem. B* **2004**, *108*, 13058.
(19) Kotlyar, A. B.; Borovok, N.; Molotsky, T.; Cohen, H.; Shapir, E.; Porath, D. *Adv. Mater.* **2005**, in press.
(20) Weizman, H.; Tor, Y. *J. Am. Chem. Soc.* **2001**, *123*, 3375−3376.
(21) Vanderbilt, D. *Phys. Rev. B* **1990**, *41*, 7892−7895.
(22) Corni, S.; De Rienzo, F.; Di Felice, R.; Molinari, E. *Int. J. Quantum Chem.* **2005**, *102*, 328−342.
(23) Elstner, M.; Hobza, P.; Frauenheim, T.; Suhai, S.; Kaxiras, E. *J. Chem. Phys.* **2001**, *114*, 5149−5155.
(24) Sugiyama, H.; Saito, I. *J. Am. Chem. Soc.* **1996**, *118*, 7063−7068.
(25) Di Felice, R.; Calzolari, A.; Molinari, E.; Garbesi, A. *Phys. Rev. B* **2001**, *65*, 045104.
(26) According to a purely one-particle picture, one would instead expect the highest edge of the occupied levels to be determined by the majority-spins (unpaired occupation).
(27) Gervasio, F. L.; Carloni, P.; Parrinello, M. *Phys. Rev. Lett.* **2002**, *89*, 108102.
(28) Di Felice, R.; Alexandre, S. S.; Calzolari, A.; Garbesi, A.; Soler, J. M. **2005**, unpublished.
(29) The DFT total energy of the FM state is lower than that of the AM state by a few tens of meV/spin, which in principle could give a rough estimate of the magnetic ordering and spin−spin coupling depending on the temperature. However, we believe that the natural environment around the base-plane stack and edge effects in the finite real polymers are relevant in determining the ultimate energetical stability. Furthermore, such tiny energy values are not accurate within the adopted computational technique and cannot be used for a predictive interpretation of experimental conditions.
(30) To compare the energy levels of the ferromagnetic and antiferromagnetic phases, the eigenvalues of the lowest occupied orbitals have been aligned. Hence, the energies given for the electron states of the antiferromagnetic wire can be located on the same scale of the plot in Figure 3 (see Supplementary Information).
(31) Barnett, R. N.; Cleveland, C. L.; Joy, A.; Landmann, U.; Schuster, G. B. *Science* **2001**, *294*, 567−571.